

Supplementary Information

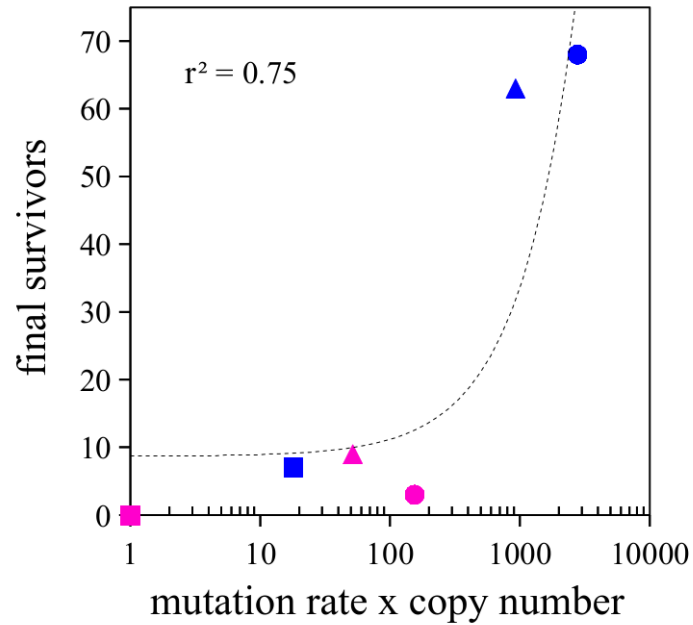


Figure S1. Correlation between the final number of survivors and the estimated product of mutation rate and *bla*_{TEM-1} copy number. Mutation rate was estimated by fluctuation test to rifampicin resistance (n=12, Jones median estimator); copy number was considered 1 for the single-copy and 18 for the multiple-copy setting. Dots correspond to wild-type (squares), *ΔmutH* (circles) and *ΔmutT* (triangles) lineages; carrying either one (pink) or multiple (blue) copies of the gene coding for the beta-lactamase TEM-1. The linear regression fit (dashed line) and its coefficient of determination are also shown.

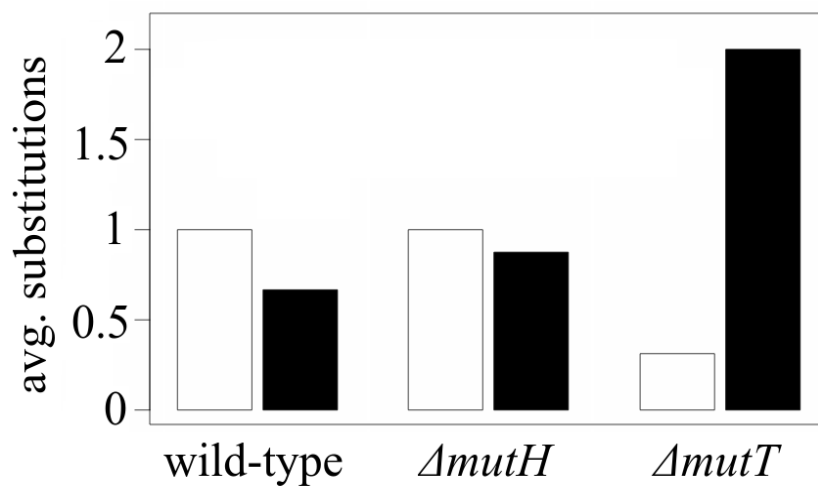


Figure S2. Genotypic profiles of high-resistance isolates from wild-type and mutator populations. Bars represent the average number of substitutions per clone observed in TEM-1 (white) and PBP3 (black) among end-point isolates from plasmid-carrying lineages that survived until the end of the experiment (MIC \geq 64mg/L). The figure shows how the $\Delta mutT$ background compensated for its inability to elevate adaptive substitutions in TEM-1 by exploiting adaptive pathways within PBP3.

Strain	Plasmid	Level ¹	POR ²	PUM ²	EryS ²	<i>acrA</i> ³	<i>acrB</i>	<i>acrR</i>	<i>envZ</i>	<i>ompR</i>	<i>ompF</i>	<i>ompC</i>
<i>ΔmutT</i>	no	0.5	1	1	0	-	W634G	E67S	H333P	-	-	L361R
<i>ΔmutH</i>	no	64	1	1	0	-	W634G	F52C	-	Y5D	-	-

1: CT concentration (in mg/mL) at which the clone was isolated

2: Labels denote absence (0) or presence (1) of altered porins (POR), increased efflux (PUM) and erythromycin hypersusceptibility (EryS). See Material and Methods for details.

3: Observed aminoacid substitution at the specified locus

Table S1. Non-synonymous mutations in loci involved in β -lactam efflux and permeability in two independent strains with positive phenotypes

Table S3. Alleles of proteins TEM-1 and PBP3 from the collection of end-point isolates

allele	substitutions	wild-type	$\Delta mutH$	$\Delta mutT$	total
FtsI-1	R167C, A475V		1		1
FtsI-2	R167C, I532L		1		1
FtsI-3	N255S, V313M		1		1
FtsI-4	A257V		1		1
FtsI-5	A257V, L369F		1		1
FtsI-6	G270R, G306V	1			1
FtsI-7	G306V	1			1
FtsI-8	G306V, L369F			1	1
FtsI-9	V309A, L369F		1		1
FtsI-10	P311A	1			1
FtsI-11	P311S		1		1
FtsI-12	V313M		1		1
FtsI-13	V313G, L369F, I532L			3	3
FtsI-14	V314G			1	1
FtsI-15	V314G, I532L			3	3
FtsI-16	M315L, L369F, I532L			1	1
FtsI-17	A317V		2		2
FtsI-18	A317V, N361S		1		1
FtsI-19	A317V, K366E, A498V		1		1
FtsI-20	L318W, I532L			1	1
FtsI-21	I336S, I532L			3	3
FtsI-22	I336S, L369F, I532L			1	1
FtsI-23	L350V, L369F			1	1
FtsI-24	L350F, N390L			1	1
FtsI-25	V355G			1	1
FtsI-26	N361S		2		2
FtsI-27	S365F		2		2
FtsI-28	S365F, A498V		1		1
FtsI-29	S365F, L369F			1	1
FtsI-30	A368E	1			1
FtsI-31	A368E, A370V		1		1
FtsI-32	L369F, V423G, I532L			1	1
FtsI-33	L369F, V467G, I532L			1	1
FtsI-34	L369F, L393V, I532L			1	1
FtsI-35	A413V		1		1
FtsI-36	G478 Δ	1			1
FtsI-37	A492T		1		1
FtsI-38	A498V		1		1
FtsI-39	I532	1	1	4	6
TEM-15	E104K, G238S		1		1
TEM-52	E104K, M182T, G238S		2		2
TEM-112	H153R, G238S		1		1
TEM-12	R164S	1			1
TEM-19	G238S	5	6	5	16